http://www.kidney-international.org

Vascular endothelial growth factor-C and -D are involved in lymphangiogenesis in mouse unilateral ureteral obstruction

Ae S. Lee[1], Jung E. Lee[1], Yu J. Jung[1], Duk H. Kim[1], Kyung P. Kang[1], Sik Lee[1], Sung K. Park[1], Sang Y. Lee[2], Myung J. Kang[3], Woo S. Moon[3], Hyung J. Kim[4], Young B. Jeong[4], Mi J. Sung[5] and Won Kim[1]

[1]Department of Internal Medicine and Institute for Medical Sciences, Chonbuk National University Medical School, Jeonju, Korea; [2]Department of Diagnostic Radiology, Chonbuk National University Medical School, Jeonju, Korea; [3]Department of Pathology, Chonbuk National University Medical School, Jeonju, Korea; [4]Department of Urology, Chonbuk National University Medical School, Jeonju, Korea and [5]Food Function Research Division, Korea Food Research Institute, Sungnam, South Korea

Lymphatic remodeling in inflammation has been found in tracheal mycoplasma infection, human kidney transplant, skin inflammation, peritonitis, and corneal inflammation. Here we investigated lymphangiogenesis in fibrotic area in unilateral ureteral obstruction, a model of progressive renal fibrosis, and evaluated the roles of vascular endothelial growth factor (VEGF)-C and -D in the obstructed kidney. Compared to sham-operated mice, the number of LYVE-1-positive lymphatic vessels, the proliferation of LYVE-1-positive lymphatic endothelial cells, along with VEGF-C and -D mRNA expression were all significantly increased following ureteral obstruction. Depletion of macrophages with clodronate decreased lymphangiogenesis in the obstructed kidney. VEGF-C expression was higher in M2- than in M1-polarized macrophages from bone marrow–derived macrophages, and also increased in Raw 264.7 or renal proximal tubule cells by stimulation with TGF-β1 or TNF-α. VEGF-D reversed the inhibitory effect of TGF-β1 on VEGF-C-induced migration, capillary-like tube formation, and proliferation of human lymphatic endothelial cells. Additionally, the blockade of VEGF-C and VEGF-D signaling decreased obstruction-induced lymphangiogenesis. Thus, VEGF-C and VEGF-D are associated with lymphangiogenesis in the fibrotic kidney in a mouse model of ureteral obstruction.

Kidney International (2012) **83,** 50–62; doi:10.1038/ki.2012.312; published online 29 August 2012

KEYWORDS: fibrosis; lymphangiogenesis; macrophages; renal tubule; unilateral ureteral obstruction

Correspondence: *Won Kim, Department of Internal Medicine and Institute for Medical Sciences, Chonbuk National University Medical School, 634-18, Keum-Am dong, Jeonju 560-180, Korea. E-mail: kwon@jbnu.ac.kr*

Received 22 December 2010; revised 5 June 2012; accepted 6 July 2012; published online 29 August 2012

A typical function of lymphatic vessels is the regulation of fluid in interstitial space and transport of immune cell and nutrients.[1] The lymphatic system is involved in many pathological conditions such as tumor metastasis, wound healing, and lymphedema. Recently, the lymphangiogenesis in acute inflammatory conditions has been demonstrated in tracheal myocoplasma infection,[2] skin inflammation,[3] peritonitis,[4,5] and corneal inflammation.[6] Lymphangiogenesis in acute airway inflammation may be associated with relief of mucosal edema, and intraperitoneal lipopolysaccharide administration induces lymphangiogenesis in the diaphragm.[2,5]

Macrophages have an important role in inflammatory-induced lymphangiogenesis. Macrophages are involved in vascular endothelial growth factor (VEGF)-A–induced inflammatory neovascularization in cornea.[7] Tracheal macrophages after mycoplasma infection also express VEGF-C and VEGF-D that increase lymphatics.[2] Studies have demonstrated that the expression of VEGF-C in lymphatic vessel endothelial hyaluronan receptor (LYVE)-1–positive and CD11b-positive macrophages has a critical role in acute skin inflammation and lipopolysaccharide-induced peritoneal inflammatory lymphangiogenesis.[3,5] These observations have indicated that lymphangiogenic factors from macrophages are actively involved in lymphangiogenesis in acute inflammatory conditions. However, the function of macrophages may be different according to the classically activated M1 and alternatively activated M2 macrophages. Until now, the role of polarized macrophages during lymphangiogenesis remains unknown.

There is also a growing body of evidence that lymphatic vascular remodeling is increased in chronic fibrotic conditions.[3–5,8,9] Lymphatic endothelial proliferation has been detected in tubulointerstitial fibrotic regions in rat remnant kidney model,[10] and lymphangiogenesis occurred at the site of tubulointerstitial lesions and strongly correlated

with areas of fibrosis in human kidney transplant.[9] Recently, El-Chemaly *et al.*[8] have demonstrated that lymphangiogenesis in idiopathic pulmonary fibrosis, a chronic progressive disease, is contributed by CD11b-positive macrophages and hyaluronic acid. However, there are few data about the lymphangiogenesis in unilateral ureteral obstruction (UUO) mice, a type of progressive renal fibrosis model.

In this study, we investigated lymphangiogenesis in a mouse model of UUO and evaluated the roles of macrophages and renal proximal tubules as a source of VEGF-C in

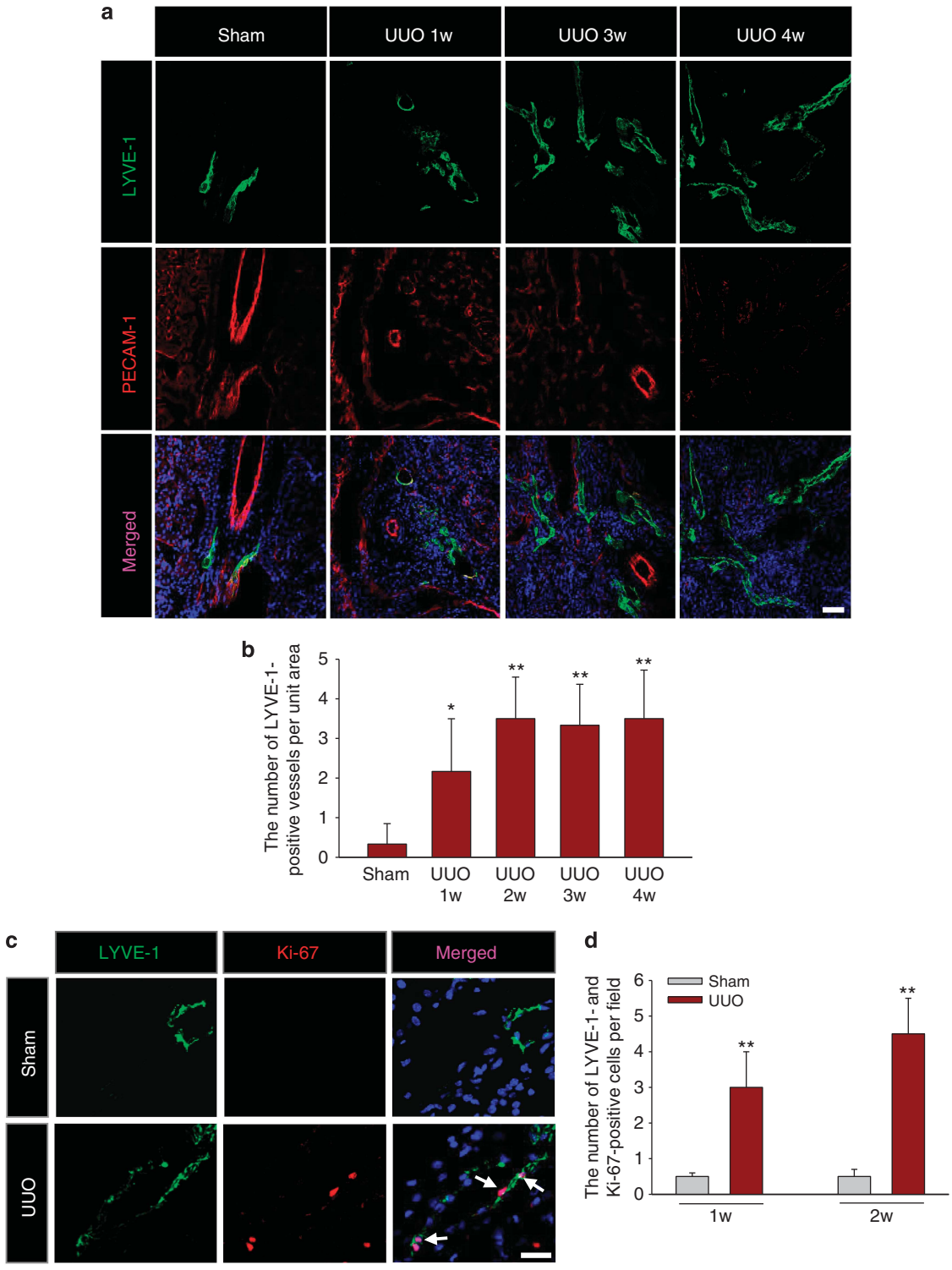

Figure 1 | For caption please refer page 52.

UUO-induced lymphangiogenesis. We also investigated the roles of VEGF-D in obstructed kidney. The results showed that the density of proliferating lymphatic endothelial cells was increased after ureteral obstruction, and that macrophages and proximal renal tubules were sources of VEGF-C in UUO-induced lymphangiogenesis. VEGF-D also contributed to lymphangiogenesis in UUO kidney.

RESULTS

The number of LYVE-1-positive lymphatic vessels is increased in the obstructed kidney

In the whole kidney image obtained by recombination of sagittal sections, LYVE-1-positive lymphatics were mostly located around platelet endothelial cell adhesion molecule-1 (PECAM-1)–positive renal vessels in the medullary portion from sham-operated kidney (Supplementary Figure S1a online). After 1 or 2 weeks of UUO, ureteral obstructed kidney showed an increase in LYVE-1-positive lymphatic vascular endothelial cell density with contracted renal parenchyma and dilated renal pelvis (Supplementary Figures S1b and c). After 4 weeks of UUO, LYVE-1-positive lymphatics were further dilated in the medullary portion of the kidney and detected abundantly in fibrotic renal parenchyma in the cortex, with more thinning of renal parenchyma and more dilated renal pelvis (Supplementary Figure S1d online). PECAM-1 was expressed not only on the endothelium of blood vessels but also on the endothelium of some lymphatic vessels (Figure 1a and Supplementary Figure S1 online). In sham-operated kidney, LYVE-1-positive lymphatics were seen only in the surrounding renal arteries and arterioles (Figure 1a). The number of LYVE-1-positive vessels in the renal cortex was increased from 1 week after UUO compared with sham-operated mice (Figure 1a and b).

Proliferation of LYVE-1-positive lymphatic vessels in UUO kidney

To determine whether LYVE-1-positive lymphatic endothelial cells are proliferating in UUO or sham-operated kidney, we stained kidney sections with Ki-67, a marker of cell proliferation, and LYVE-1. In the sham-operated kidney, most LYVE-1-positive endothelial cells were rarely stained with Ki-67 (Figure 1c and d). In the UUO kidney, the numbers of LYVE-1- and Ki-67-positive cells per unit area were increased in the renal cortex, showing approximately 3.1- and 4.5-fold increase over the sham-operated kidney after 1 and 2 weeks of UUO, respectively (Figure 1c and d).

VEGFR-3, podoplanin, and Prox-1 are coexpressed on LYVE-1-positive endothelial cells

To evaluate whether LYVE-1-positive endothelial cells were costained with other lymphatic markers, kidney sections from UUO mice were immunostained with an antibody against VEGF receptor-3 (VEGFR-3), podoplanin, Prox-1, or LYVE-1. LYVE-1-positive lymphatic vascular endothelial cells were also immunostained with VEGFR-3 after 1 week of UUO. A lymphatic endothelial cell transcription factor, Prox-1, was also detected in the nucleus of the LYVE-1- and podoplanin-positive lymphatic endothelial cells (Supplementary Figures S2a and b online).

LYVE-1-positive vascular lymphatics remodeling correlates with the severity of interstitial fibrosis

The severity of renal interstitial fibrosis progressively increased after UUO (Figure 2). To assess whether the change of vascular density of LYVE-1-positive lymphatics is correlated with the progression of renal fibrosis, the kidney sections from sham-operated and UUO mice were stained with a LYVE-1 antibody, and with hematoxylin and eosin and Masson's trichrome stains. In sham-operated kidney, the presence of fibrotic lesions was rare, and LYVE-1-positive lymphatics were only found around the renal arteries and arterioles (Figure 2a). In UUO kidney, fibrotic lesions in the cortex were progressively increased after UUO in Masson's trichrome–stained kidney sections. Vascular density of LYVE-1-positive lymphatics was increased in a time-dependent manner (Figure 2a and b). Vasculature of LYVE-1-positive lymphatics was significantly increased in the cortical interstitial fibrotic area after UUO, which was not found in sham-operated kidney (Figure 2a and b). The increase in renal cortical fibrosis was positively correlated with the increase in the LYVE-1-positive lymphatics in unit area ($r^2 = 0.772$, $P < 0.01$).

Gene expression correlates with lymphangiogenesis in UUO kidney

To identify changes in lymphangiogenic growth factors, we performed quantitative real-time reverse-transcription

Figure 1 | Confocal microscopic images in sham-operated and unilateral ureteral obstruction (UUO) mouse kidney 1, 2, 3, and 4 weeks (w) after obstruction. (**a**) Double immunostaining of lymphatic vessel endothelial hyaluronan receptor-1 (LYVE-1) and platelet endothelial cell adhesion molecule-1 (PECAM-1) was carried out using sham-operated (Sham) and ureteral obstructed kidneys 1w, 3w, and 4w after operation. UUO kidney demonstrated abundant and enlarged LYVE-1-positive lymphatic vessels 1w, 3w, and 4w after obstruction. PECAM-1-positive vascular density was slightly increased in mice 2w after ureteral obstruction compared with sham-operated mice. Thereafter, PECAM-1-positive vascular density was gradually decreased. Bar = 50 μm. (**b**) The number of LYVE-1-positive lymphatic vessels per unit area in sham-operated and fibrotic kidney ($n = 6$ in each group). Bars represent mean ± s.d. *$P < 0.05$ versus sham; **$P < 0.01$ versus sham. (**c**) Immunofluorescence study of LYVE-1 and Ki-67 in kidney. Kidneys from mice that underwent sham or UUO operation were collected 1w after operation. Tissues were fixed in 4% formaldehyde solution, and frozen sections were then stained with LYVE-1 and Ki-67 antibodies. Arrows indicate proliferating lymphatic endothelial cells. Bar = 20 μm. (**d**) Quantification of the number of LYVE-1- and Ki-67-positive cells in sham-operated or UUO kidney 1w and 2w after operation. Note that the number of cells that are coimmunoreactive for LYVE-1 and Ki-67 in UUO kidney was increased significantly compared with that of the kidney after sham operation ($n = 6$ in each group). Data are expressed as mean ± s.d. **$P < 0.01$ versus sham in each time.

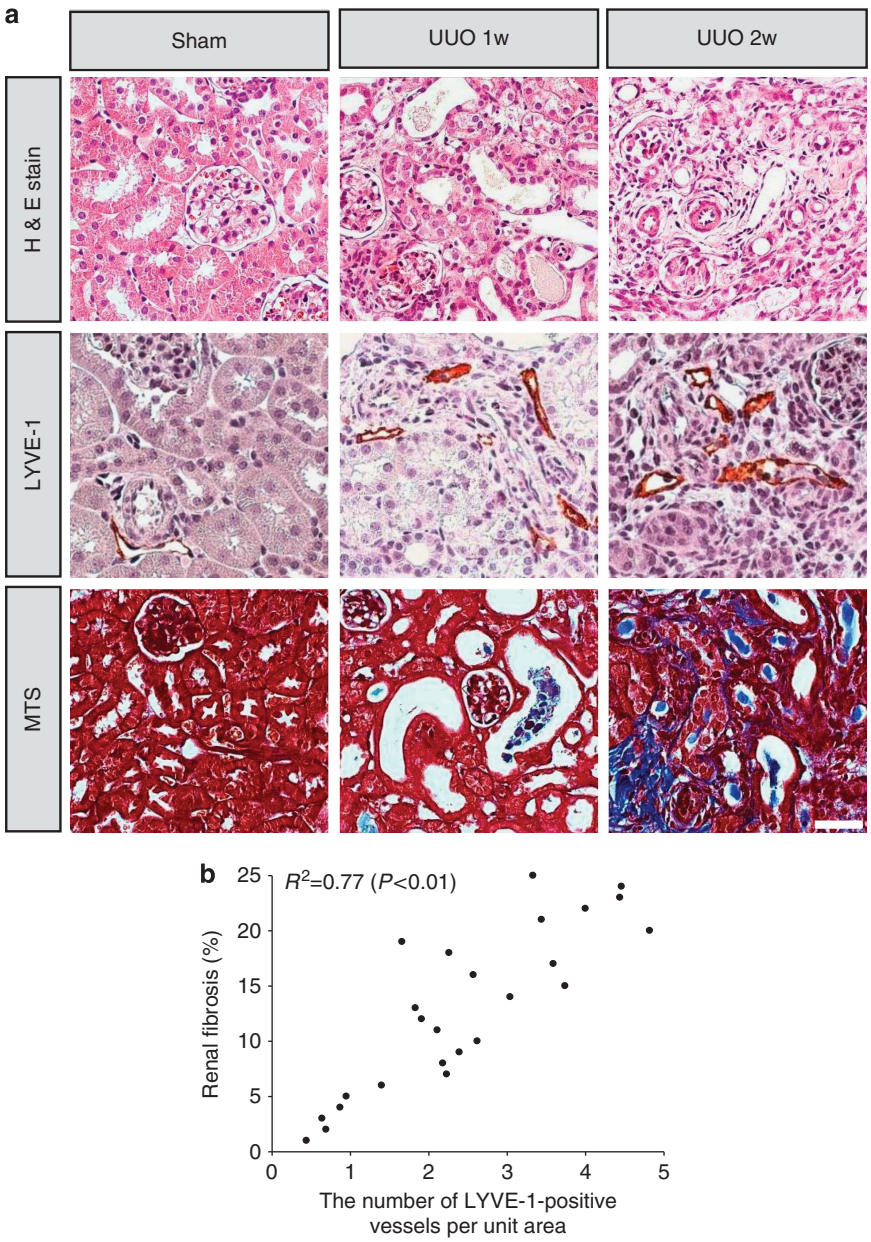

Figure 2 | Immunohistochemical study of lymphatic vessel endothelial hyaluronan receptor-1 (LYVE-1), hematoxylin and eosin (H&E), and Masson's trichrome (MTS) stain on normal and fibrotic kidney sections after ureteral obstruction. (**a**) Kidneys from mice that underwent sham operation or ureteral obstruction were collected 1 and 2 weeks (w) after operation. Bar = 50 μm. (**b**) Correlation between the number of LYVE-1-positive lymphatic vessels and renal cortical interstitial fibrosis defined as percentage of MTS-positive fibrotic area ($n = 6$ in each group). Note that there is a positive correlation between the number of LYVE-1-positive lymphatic vessels and fibrotic area in fibrotic kidney after ureteral obstruction. UUO, unilateral ureteral obstruction.

PCR (qRT-PCR).[7,11–16] As shown in Figure 3, the mRNA expression of angiopoietin (Ang)1, VEGF-C, and VEGF-D was increased 6-, 13-, and 6-fold 1 week after UUO, respectively, compared with sham-operated kidney. The increased mRNA level of VEGF-C and VEGF-D was sustained up to 4 weeks, whereas the increased mRNA level of Ang1 was decreased after 3 weeks of UUO. The mRNA expression of VEGF-A was decreased 3 and 4 weeks after UUO (Figure 3a). To evaluate changes in VEGF-C mRNA level in glomeruli and renal tubules, we isolated glomeruli from the kidney 1 week after UUO and performed qRT-PCR. Our qRT-PCR data demonstrated that the level of VEGF-C mRNA in renal tubules was significantly increased after UUO operation compared with the level of sham operation (Figure 3b). However, the VEGF-C mRNA level in glomeruli was not significantly changed compared with the level in sham-operated mice (Figure 3b).

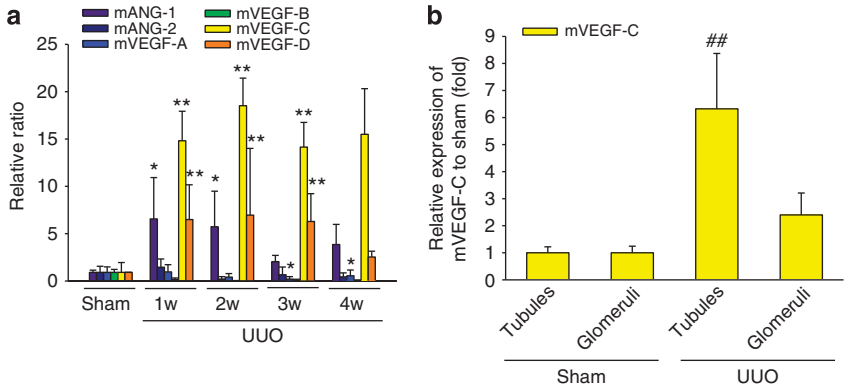

Figure 3 | Lymphangiogenic gene expression analysis by quantitative real-time reverse transcription PCR. (**a**) Fold changes of gene expression are relative to sham at 1, 2, 3, and 4 weeks (w) after operation. The expression of mouse angiopoietin-1 (mAng1), mouse vascular endothelial growth factor (mVEGF)-C, and VEGF-D in unilateral ureteral obstruction (UUO) kidney was significantly increased compared with sham-operated mice ($n = 3$ in each group). (**b**) Relative expression of VEGF-C mRNA in renal tubules and glomeruli 1w after UUO ($n = 3$ in each group). Bars represent mean ± s.d. $^{*}P < 0.05$ versus sham; $^{**}P < 0.01$ versus sham; $^{\#\#}P < 0.01$ versus tubules in sham.

Macrophage depletion decreases UUO-induced lymphangiogenesis and renal injury

VEGF-C expression has been shown to increase in macrophages in acute inflammation.[3–5] We therefore evaluated the role of macrophages in lymphangiogenesis in UUO kidney by depletion of the cells with liposomal clodronate. Administration of liposomal clodronate reduced the number of F4/80-positive macrophages in the kidney by approximately 92% and markedly inhibited UUO-induced lymphangiogenesis by approximately 85% (Figure 4a–c). Histological analysis showed that depletion of macrophages reduced renal interstitial fibrosis in UUO kidney (Figure 4d).

Knockdown of VEGF-C in macrophages decreases the UUO-induced lymphangiogenesis

We evaluated the effect of adoptive VEGF-C knockdown macrophage transfer on renal lymphangiogenesis after UUO using VEGF-C-specific short hairpin RNA lentiviral vector (VEGF-C shRNA). VEGF-C shRNA– or non-target shRNA–transfected bone marrow–derived macrophages were transferred into severe combined immunodeficiency mice, and the lymphangiogenesis in the UUO kidney was evaluated. Immunofluorescence study demonstrated that VEGF-C shRNA–transfected macrophages significantly decreased the UUO-induced increase of LYVE-1-positive lymphatic vessels (Supplementary Figure S3 online).

Expression of VEGF-C dominantly increased in alternatively activated M2 macrophages

Although the number of macrophages significantly increases within UUO kidney and has an important role in UUO-induced lymphangiogenesis in our experiment, macrophages are heterogeneous in function and include classically activated M1 and alternatively activated M2 macrophages. It has been suggested that M2-polarized macrophages promote angiogenesis and lymphangiogenesis in tumor.[17–19] These findings led us to assess the expression and localization of VEGF-C in alternatively activated M2 macrophages from UUO kidney and primary-cultured bone marrow–derived macrophages. To evaluate the VEGF-C expression in M2 or M1 macrophages in UUO kidney, we immunostained the UUO kidney sections using an antibody against an M2-polarized macrophage marker, mannose receptor (CD206), or an M1-polarized macrophage marker, inducible nitric oxide synthase (iNOS). Immunofluorescent findings showed that about 33 ± 4% of CD206-positive cells were costained with VEGF-C in kidney sections after 1 week of UUO (Figure 5a). iNOS-positive macrophages also expressed VEGF-C (Figure 5b). We also examined the changes of VEGF-C expression in M1- or M2-polarized macrophages *in vitro*. Bone marrow–derived macrophages were stimulated with interferon-γ or interleukin (IL)-4 for 48 h to induce the M1 or M2 macrophage phenotype and immunoblotting was performed with iNOS and an M2-polarized macrophage marker, arginase-1. Treatment of macrophages with interferon-γ increased the expression of iNOS, and treatment with IL-4 increased the expression of arginase-1 (Figure 5c and d). The expression of VEGF-C protein in M2-polarized macrophages was higher than in M1-polarized bone marrow–derived macrophages (Figure 5e).

TGF-β1 or TNF-α increases VEGF-C expression in Raw 264.7 cells

We found that the transforming growth factor (TGF)-β1 level in UUO kidney was significantly higher than that in sham-operated kidney in this experiment (Supplementary Figure S4 online). As TGF-β1 and tumor necrosis factor (TNF)-α have a major role in renal fibrosis, we evaluate whether stimulation of macrophages with TGF-β1 or TNF-α increases the expression of VEGF-C protein in Raw 264.7 cells, an established macrophage cell line.[5,20–22] Treatment with TGF-β1 at concentrations of 10 and 20 ng/ml increased the expression of VEGF-C by approximately 2.6- and

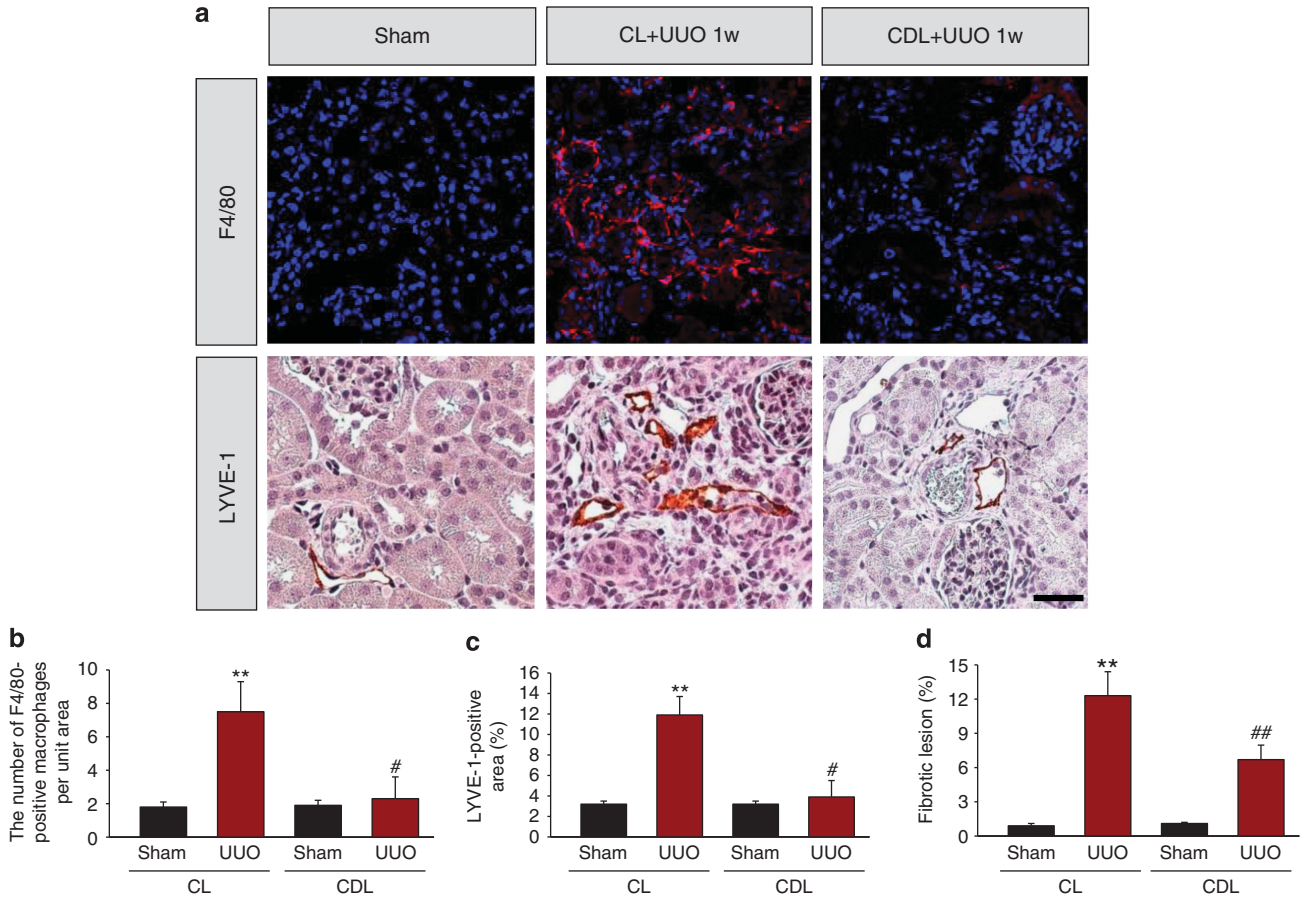

Figure 4 | Effect of macrophage depletion and blockade of vascular endothelial growth factor (VEGF)-C on unilateral ureteral obstruction (UUO)–induced lymphangiogenesis in the kidney. For systemic depletion of macrophages, clodronate liposome (CDL, 50 mg/kg) was administered through the peritoneum 1 day before operation and every second day before collecting kidney sample. Empty control liposome (CL) was injected as a control. Kidneys from mice that underwent sham or UUO operation were collected 1 week after operation. (**a**) Tissues were fixed in 4% formaldehyde solution, and kidney sections were then stained with F4/80 and lymphatic vessel endothelial hyaluronan receptor-1 (LYVE-1) antibody. Note that administration of CDL markedly reduced the number of F4/80-positive macrophages in the kidney and also suppressed lymphangiogenesis induced by ureteral obstruction. (**b**) The number of F4/80-positive macrophages in unit area of the kidney. The number of F4/80-positive macrophages in sham-operated or UUO kidney was measured in each given area (3.64 mm^2, $n=4$ in each group). Bars represent mean ± s.d. (**c**) Area density of LYVE-1-positive lymphatic endothelial cells in sham-operated and fibrotic kidney ($n=4$ in each group). Bar graph shows the area density of the positively stained area to the total field. (**d**) Fibrosis of the sham-operated and UUO kidneys ($n=4$ in each group). Bars represent mean ± s.d. $^{**}P<0.01$ versus sham + CL; $^{\#}P<0.05$ versus UUO + CL; $^{\#\#}P<0.01$ versus UUO + CL.

2.1-fold, respectively (Supplementary Figure S5a online). Treatment of Raw 264.7 cells with TGF type 1 receptor inhibitors (LY364947 and SD208) and an inhibitor of TGF-β superfamily type I activin receptor–like kinase (ALK) receptors ALK4, 5, and 7 (SB431542) significantly decreased TGF-β1-induced VEGF-C production (Supplementary Figure S5b online). We also investigated the effects of TNF-α on VEGF-C production in Raw 264.7 cells. TNF-α at a concentration of 10 ng/ml increased VEGF-C expression by approximately 3.1-fold compared with control buffer–treated Raw 264.7 cells (Supplementary Figure S5c). These results indicate that TGF-β1 or TNF-α increases VEGF-C production and that TGF type 1 receptor and TGF-β superfamily type I ALK receptors 4, 5, and 7 are involved in TGF-β1-mediated VEGF-C expression.

TGF-β1 or TNF-α increases VEGF-C expression in proximal tubular cells

As VEGF-C from activated macrophages is involved in lymphangiogenesis in ureteral obstructed kidneys, we explored other sources of VEGF-C in the UUO kidney. Thus, we immunostained kidney sections with anti-VEGF-C and aquaporin 1 antibodies. Immunofluorescence findings showed that VEGF-C expression in UUO kidney was increased in renal tubules compared with sham-operated kidney, and VEGF-C-positive renal tubule cells were costained with aquaporin 1, a marker of proximal tubule in UUO kidney (Figure 6a). Aquaporin 1 was expressed on the apical and basolateral membrane of the proximal tubule in sham-operated and UUO kidney as previously reported.[23,24] To evaluate changes of VEGF-C protein expression in mouse

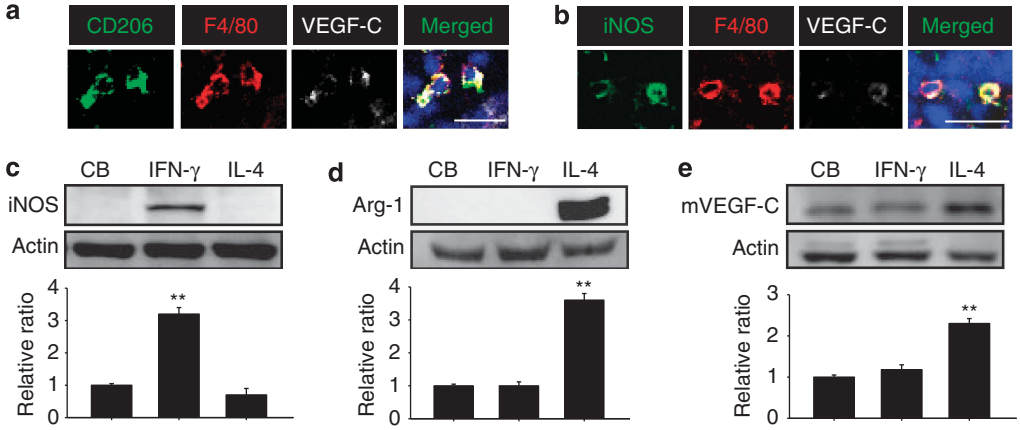

Figure 5 | Immunofluorescence of mannose receptor (CD206), inducible nitric oxide synthase (iNOS), and vascular endothelial growth factor (VEGF)-C in kidney and immunoblot analyses of VEGF-C in bone marrow–derived macrophages. (**a**, **b**) Unilateral ureteral obstruction (UUO) kidneys were harvested 1 week (w) after operation. Tissues were fixed in 4% formaldehyde solution, and frozen sections were then stained with anti-F4/80, anti-iNOS, anti-CD206, and anti-VEGF-C antibodies. Nuclei were stained with DAPI (4′,6-diamidino-2-phenylindole; blue color). Note that VEGF-C was costained with F4/80- and CD206-positive cells, and also with F4/80- and iNOS-positive cells in UUO kidney. Bar = 20 μm. (**c**–**e**) The bone marrow–derived macrophages were collected and treated with interferon (IFN)-γ or interleukin (IL)-4 for 48 h. Blots (top) were probed with an anti-VEGF-C, anti-iNOS, or anti-arginase (Arg)-1 antibody. iNOS was used as a marker of M1 macrophage and Arg-1 as a marker of M2 macrophage. The membrane was stripped and reprobed with an anti-actin antibody to control for protein loading in each lane. Note that the expression of VEGF-C in bone marrow–derived M2 macrophages after stimulation with IL-4 was significantly higher than that of M1 macrophages after stimulation with IFN-γ ($n = 4$). Bars represent mean ± s.d. $^{**}P < 0.01$ versus control buffer (CB).

proximal tubular (MPT) and HK2 cells, established mouse and human proximal tubular cell lines, respectively, we stimulated MPT and HK2 cells with TGF-β1 or TNF-α for 24 h and performed immunoblot analysis. Treatment with TGF-β1 (10 ng/ml) or TNF-α (10 ng/ml) increased VEGF-C expression by approximately 2.6- or 2.9-fold, respectively, compared with control buffer–treated MPT cells (Figure 6b and c). Treatment with TGF-β1 (10 ng/ml) or TNF-α (10 ng/ml) increased VEGF-C expression by about 3.5- or 3.7-fold, respectively, compared with control buffer–treated HK2 cells (Figure 6d and e). We also found that LY364947, SD208, and SB431542 significantly decreased TGF-β1-induced VEGF-C production in MPT cells (Figure 6f). These data suggest that TGF-β1 increases VEGF-C production through the TGF type 1 receptor and TGF-β type I receptors ALK4-, 5-, and 7-dependent signal pathway in MPT cells.

VEGF-D reverses the inhibitory effect of TGF-β1 on VEGF-C-induced *in vitro* lymphangiogenesis

TGF-β1 is a negative regulator in lymphangiogenesis and inhibits lymphatic regeneration during wound repair.[25–27] Tube formation, migration, and proliferation of lymphatic endothelial cells are important components in *in vitro* lymphangiogenesis. We evaluated the effect of TGF-β1 on VEGF-C-induced *in vitro* lymphangiogenesis using human lymphatic endothelial cells (hLECs). In line with previous data, treatment of hLECs with TGF-β1 significantly decreased VEGF-C-induced tube formation, migration, and proliferation (Figure 7a–d).[26] We also found that mRNA and protein expression of VEGF-C and VEGF-D increased in UUO kidney compared with sham-operated mice (Figures 3a, 7e and f). We further evaluated whether treatment with VEGF-D ameliorates the inhibitory effect of TGF-β1 on VEGF-C-induced capillary-like tube formation, migration, and proliferation of hLECs. VEGF-D significantly reversed the suppressive effect of TGF-β1 on VEGF-C-induced capillary-like tube formation, migration, and proliferation of hLECs (Figure 7a–d).

Blockade of VEGF-C and VEGF-D decreases UUO-induced lymphangiogenesis

The ligands of VEGFR-3 are known as VEGF-C and VEGF-D.[12,28] To ascertain the role of VEGF-C and VEGF-D in UUO-induced lymphangiogenesis, we blocked the effect of VEGF-C and VEGF-D using adenovirus encoding the soluble extracellular domain of VEGFR-3 (Ad-sVEGFR3).[29] Treatment of UUO-operated mice with Ad-sVEGFR3 decreased the UUO-induced increase of the number of lymphatic vessels in the renal cortex compared with mice treated with adenovirus-encoding β-galactosidase (Ad-β-galactosidase; Figure 7g). The sham-operated mice treated with the Ad-sVEGFR3 showed no signicant differences from the sham-operated mice treated with Ad-β-galactosidase.

Lymphatic remodeling in fibrotic human kidney after ureteral obstruction

To evaluate whether there is lymphatic vascular remodeling in fibrotic human kidney after ureteral obstruction due to ureteral cancer, the kidney sections were immunostained with anti-D2-40 (human lymphatic vascular marker) antibody.

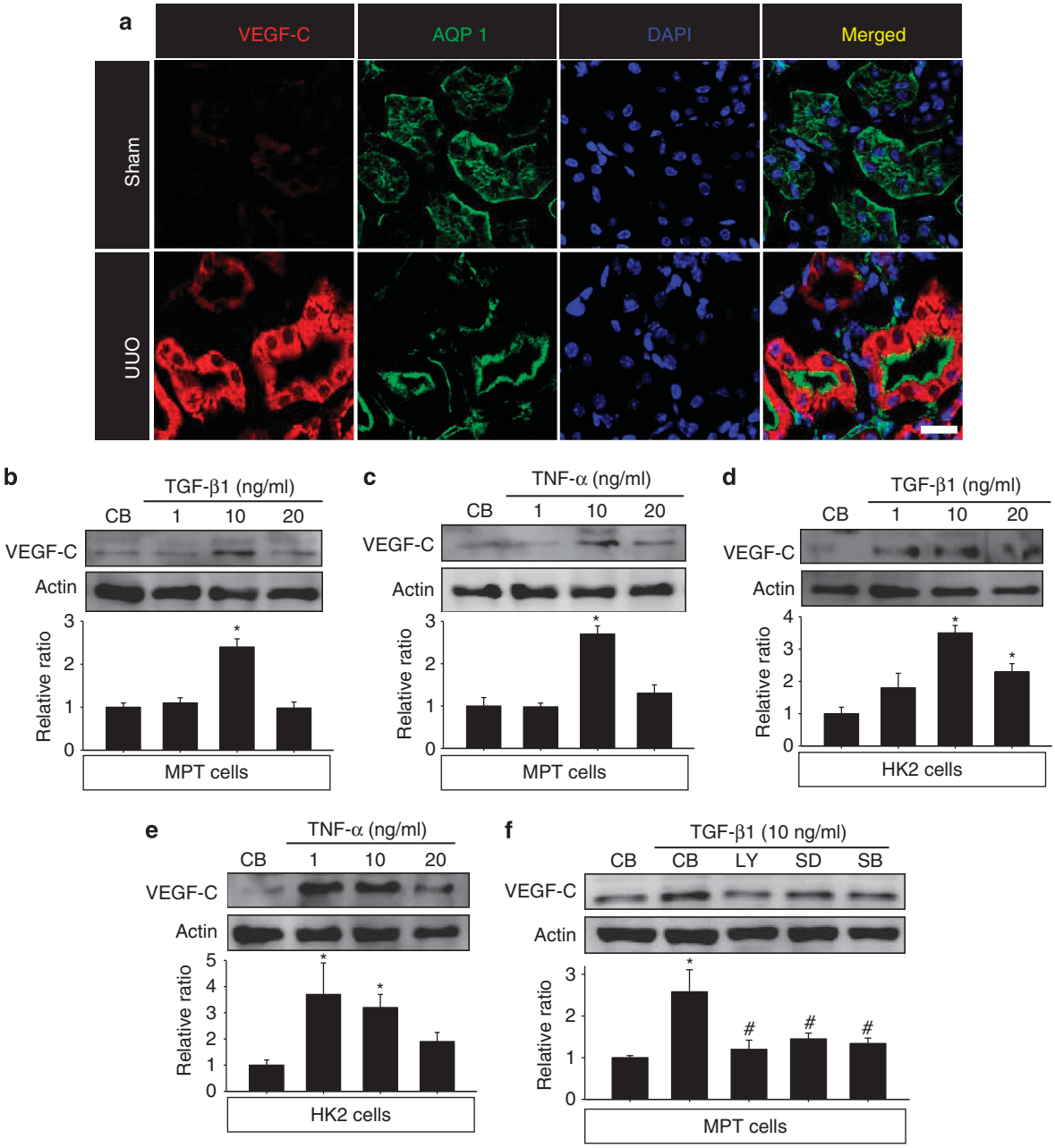

Figure 6 | Immunofluorescence of aquaporin 1 (AQP1) and vascular endothelial growth factor (VEGF)-C in kidney and immunoblot analyses of VEGF-C in mouse proximal tubular (MPT) and HK2 cells. (**a**) Kidneys from mice that underwent sham operation (Sham) or unilateral ureteral obstruction (UUO) operation were collected 1 week after operation. Tissues were fixed in 4% formaldehyde solution, and frozen sections were then stained with VEGF-C. Note that the expression of VEGF-C in AQP1-positive renal tubules was increased in UUO compared with sham-operated kidney. Bar = 20 μm. (**b**, **c**) The MPT cells were treated with transforming growth factor (TGF)-β1 or tumor necrosis factor (TNF)-α at indicated concentrations for 24 h. Blots (top) were probed with an anti-VEGF-C antibody and the membrane was reprobed with an anti-actin antibody to control for protein loading in each lane. Note that the expression of VEGF-C in MPT cells after stimulation with TGF-β1 or TNF-α was significantly increased compared with that after stimulation with control buffer (CB; $n = 3$). (**d**, **e**) HK2 cells were treated with TGF-β1 or TNF-α at indicated concentrations for 24 h. Blots were probed with an anti-VEGF-C antibody and reprobed with an anti-actin antibody to control for protein loading in each lane. Note that the expression of VEGF-C in HK2 cells after stimulation with TGF-β1 or TNF-α was significantly increased compared with that after stimulation with CB ($n = 3$). (**f**) MPT cells were treated with TGF-β1 (10 ng/ml), LY364947 (LY), SD208 (SD), and SB431542 (SB) for 24 h. Blots (top) were probed with an anti-VEGF-C antibody, and the membrane was reprobed with an anti-actin antibody to control for protein loading in each lane ($n = 3$). Bars represent mean ± s.d. $^{*}P < 0.05$ versus CB; $^{\#}P < 0.05$ versus CB + TGF-β1.

In normal human kidney tissues, D2-40 positive–stained endothelium of lymphatic vascular system was located just around renal arterioles and arteries (Supplementary Figure S6 online). However, the density of D2-40-positive lymphatics in interstitial fibrotic area in ureteral obstructed human kidney was increased compared with normal kidney.

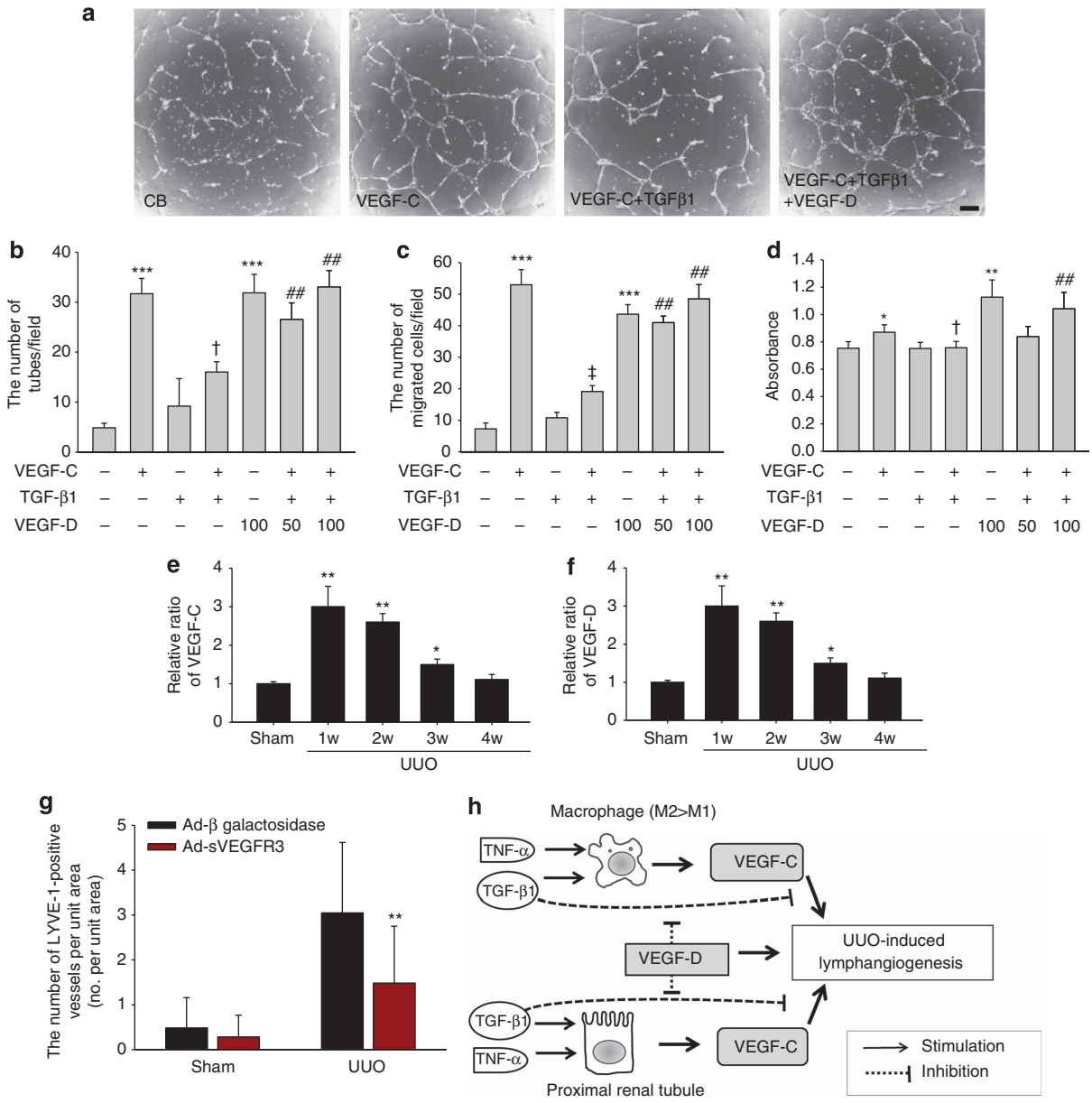

Figure 7 | Vascular endothelial growth factor (VEGF)-D reverses the inhibitory effect of transforming growth factor (TGF)-β1 on VEGF-C-induced lymphangiogenesis. (**a**) Phase-contrast photographs of capillary-like tube formation in extracellular matrix (ECM) gel. Gels were incubated for 16 h in the presence of the indicated reagents (VEGF-C 100 ng/ml, TGF-β1 10 ng/ml, and VEGF-D 50 or 100 ng/ml). Capillary-like tube formation was assayed in three-dimensional matrices of ECM gel as described in 'Materials and Methods'. Bar at lower right = 50 μm. (**b**) Quantification of capillary-like tube formation. Tube formation was quantified by the number of tubes using phase-contrast microscopy. Bars represent means ± s.d. from four independent experiments. (**c**) Migration assay, control buffer (CB), VEGF-C (100 ng/ml), TGF-β1 (10 ng/ml), and/or VEGF-D (50 or 100 ng/ml) in endothelial basal medium-2 containing 1% bovine serum albumin were placed in the bottom wells of the chamber. Cells that migrated through to the lower chamber were stained with Diff-Quik solution and counted at × 200 magnification as described in 'Materials and Methods'. Bars represent means ± s.d. from four independent experiments. (**d**) Human lymphatic endothelial cells (hLECs) were incubated with CB, VEGF-C (100 ng/ml), TGF-β1 (10 ng/ml), and VEGF-D (50 or 100 ng/ml). After the 48-h incubation period, hLEC proliferation was measured with an XTT assay. Bars represent means ± s.d. from four independent experiments. (**e**, **f**) The relative ratio of VEGF-C (**e**) and VEGF-D (**f**) was measured by enzyme-linked immunosorbent assay (ELISA). The level of VEGF-C and VEGF-D was quantified by ELISA in sham-operated or unilateral ureteral obstruction (UUO) kidneys at 1, 2, 3, and 4 weeks (w) after surgery. Results were similar in three independent experiments. (**g**) The number of LYVE-1-positive lymphatic vessels after treatment with intravenous injection of 10^9 p.f.u. adenovirus encoding the soluble extracellular domain of VEGFR-3 (Ad-sVEGFR3) or control adenovirus encoding β-galactosidase (Ad-β-galactosidase) before and 7 days after ureteral obstruction. Note that the administration of Ad-sVEGFR3 suppressed lymphangiogenesis induced by UUO. Bars represent mean ± s.d. (**h**) Schematic summary of lymphangiogenesis in the UUO model. $^{*}P<0.05$ versus CB; $^{**}P<0.01$ versus CB or sham + Ad-β-galactosidase; $^{***}P<0.001$ versus CB; $^{\dagger}P<0.05$ versus VEGF-C alone; $^{\ddagger}P<0.01$ versus VEGF-C alone; $^{\#\#}P<0.01$ versus VEGF-C + TGF-β1.

DISCUSSION

The present study has revealed that interstitial fibrosis in mouse ureteral obstructed kidney and human fibrotic kidney is accompanied by lymphangiogenesis, and that the degree of lymphangiogenesis is correlated with the severity of renal fibrosis. Identification of lymphangiogenic factors showed that mRNA level of VEGF-C and VEGF-D was specifically increased in the UUO kidney in a time-dependent manner. Our results also revealed that sources of VEGF-C were macrophages and renal tubule cells (Supplementary Figure S5 online). Supporting the observations, depletion of macrophages decreased the UUO-induced lymphangiogenesis in fibrotic kidney, and treatment of MPT and HK2 cells with TGF-β1 or TNF-α increased VEGF-C expression. VEGF-D reverses the inhibitory effect of TGF-β1 on VEGF-C-induced *in vitro* lymphangiogenesis.

VEGF-C production from activated macrophages is associated with lymphangiogenesis in inflammatory conditions.[3–5,30] In line with previous results,[21,31,32] our histological data showed that infiltration of F4/80-positive macrophages was increased in UUO kidney, and this increased infiltration of macrophages was associated with an increase in lymphatic endothelial cell density. Supporting the observation, treatment with liposomal clodronate to deplete macrophages decreased UUO-induced lymphangiogenesis. These observations suggest that macrophages have a critical role in UUO-induced lymphangiogenesis.

One of the important issues in lymphangiogenesis in renal fibrosis is the source of lymphangiogenic factors in the kidney. A recent study has indicated that VEGF-C and VEGF-D are involved in lymphangiogenesis in various inflammatory conditions.[2,3] Lymphatic vasculature remodeling has been demonstrated in tracheal mycoplasma infection, and VEGF-C or VEGF-D expression is increased in macrophages in mucosal inflammation.[2] It has been reported that lipopolysaccharide-induced acute peritoneal inflammation increases peritoneal lymphangiogenesis, and that VEGF-C and VEGF-D from LYVE-1-positive macrophages are involved in acute inflammatory lymphangiogenesis.[3,5] Supporting these findings, our qRT-PCR analysis data revealed that UUO predominantly increased the level of VEGF-C and VEGF-D mRNA in the kidney. Taken together, activated macrophages are involved in lymphangiogenesis in acute inflammation by the production and release of lymphangiogenic growth factors, and VEGF-C and VEGF-D may be a major lymphangiogenic factor in UUO-induced lymphangiogenesis.

M1-polarized macrophages are activated by T-helper 1 cytokines such as interferon-γ, IL-1, and lipopolysaccharide, and M2-polarized macrophages are activated by T-helper 2 cytokines such as IL-4 and IL-13. Animal experiments have demonstrated that there are different forms of polarization of macrophages in chronic inflammatory state, such as chemical- and pathogen-induced chronic lung inflammation[33] and adipose tissue inflammation in high-fat diet–induced obese mice.[34] Recently, it has been reported that M1 or M2 activation signals may determine the influence of VEGF production from macrophages.[17] These findings suggest that macrophage polarization may have a role in UUO-induced lymphangiogenesis. However, the effect of polarized macrophages during lymphangiogenesis has not been well defined. Our data showed that the expression of VEGF-C protein was higher in IL-4-induced M2-polarized macrophages than in interferon-γ-induced M1-polarized macrophages of bone marrow–derived cells, and the expression of VEGF-C protein in Raw 264.7 cells was also higher after M2 polarization than after M1 polarization. In addition, VEGF-C protein was expressed on M2-polarized macrophages in UUO kidney. These results indicate that alternatively activated macrophages may be involved in UUO-induced lymphangiogenesis.

We also evaluated whether VEGF-C expression increased in renal tubules after ureteral obstruction. It has been reported that lymphangiogenesis is associated with VEGF-C expression in inflammatory mononuclear cells and renal proximal tubular epithelial cells in human renal biopsy specimen.[32] Our immunofluorescence data showed that VEGF-C expression was significantly increased in renal proximal tubule cells after UUO compared with the VEGF-C expression after sham operation. To support these findings, we treated the MPT and HK2 cells with TGF-β1 or TNF-α, which have been shown to increase in the UUO mouse model.[20] We found that VEGF-C expression was significantly increased in MPT cells after stimulation with TGF-β1 or TNF-α compared with the control. Our data also demonstrated that treatment with TGF-β1 or TNF-α increased the expression of VEGF-C in HK2 cells. Taken together, TGF-β1- and TNF-α-induced VEGF-C expression in renal proximal tubules may exhibit a paracrine effect on lymphangiogenesis in renal fibrosis. However, TGF-β1 is also known to decrease lymphangiogenesis, and inhibition of TGF-β1 increases lymphatic regeneration.[26,27] We found that the expression of VEGF-C and VEGF-D lymphangiogenic factors was increased during UUO-induced renal fibrosis. Recently, it has been suggested that a coordinated expression of lymphangiogenic and anti-lymphangiogenic cytokine is linked to lymphatic function.[35] Therefore, the expression of both negative and positive lymphangiogenic regulators may have a role in UUO-induced lymphangiogenesis. Supporting the contention, our results showed that VEGF-D abolished TGF-β1-induced negative lymphangiogenenic effect and was also actively involved in UUO-induced lymphangiogenesis (Figure 7).

Although tubular atrophy is a consequence of epithelial cell apoptosis and epithelial to mesenchymal transdifferentiation, it is usually linked to interstitial fibrosis. Fibrosis presents a number of characteristic features including a chronic inflammatory reaction and an increased interstitial fibroblast and matrix accumulation.[36] The interstitial cellular response to UUO is associated with an increase of inflammatory reaction.[21] It is well known that lymphangiogenesis is associated with acute or chronic inflammation. Therefore, tubular atrophy in UUO can be linked to lymphangiogenesis

in the interstitial fibrotic area. As expressions of angiogenic or lymphangiogenic growth factors may increase during tubular atrophy and renal fibrosis after ureteral obstruction, there may be less injury of the lymphatic endothelial cells compared with renal tubule cells. During renal fibrosis with tubular atrophy, the fibrotic kidney decreases in size. Therefore, the density of lymphatic vessels in fibrotic kidney may be higher than that of renal tubular cells. The relative increase of lymphatic endothelial cells per unit area in severe renal fibrotic kidney after UUO can be one of the explanations for a mechanism in UUO-induced lymphangiogenesis.

We found that injured renal tubules in fibrotic area did not expressed VEGF-C, whereas uninjured renal tubules adjacent to the fibrotic area expressed VEGF-C. Our immunoblot data demonstrated that treatment with TGF-β1 or TNF-α increased VEGF-C expression in renal tubules. Therefore, it can be suggested that TGF-β1- or TNF-α-induced VEGF-C expression from intact renal tubules may have a paracrine effect on lymphangiogenesis in the renal fibrotic area.

Another important issue in lymphangiogenesis in renal fibrosis is whether lymphangiogenesis in fibrotic kidney is associated with a beneficial role in the destructing process of renal parenchyma after ureteral obstruction. Recently, disturbance of lymph circulation by lymphatic ligation has been shown to induce renal brosis; such changes in lymphatic flow can be a factor for renal fibrosis.[37] A study has demonstrated that fibrosis in soft tissue involves impairment in lymphatic cell proliferation and lymphatic function, and suggested that the fibrotic process decreases lymphatic repair and regeneration of normal capillary lymphatics.[38] However, Kerjaschki *et al.*[9] have demonstrated that lymphangiogenesis contributes to the export of the inflammatory cell infiltrate in human transplants.[9] In the present study, our data showed that depletion of macrophages by clodronate treatment decreased lymphatic endothelial cell density and renal tubular injury score in UUO kidney, indicating that macrophages have important roles in lymphangiogenesis and in the destructing process in renal fibrosis. However, there is a paucity of data on the functional role of renal lymphangiogenesis in renal fibrotic process, and thus further studies are needed.

In summary, our results have suggested that VEGF-C and VEGF-D have a role in lymphangiogenesis in fibrotic kidney of mice induced by UUO.

MATERIALS AND METHODS

Animal experiments: UUO model

Animal studies were reviewed and approved by the Institutional Animal Care and Use Committee of Chonbuk National University. Male C57BL/6 mice (Orient Bio, Seoul, Korea; 18–20 g body weight) were used for the UUO model with the previously described method.[21] Briefly, an incision was made in the midline of the abdomen, and the left proximal ureter was exposed and was ligated at two separate locations using 3-0 silk. Kidney samples were collected 1, 2, 3, and 4 weeks after ureteral obstruction. To block VEGF-C and VEGF-D signaling, mice were treated with intravenous injection of 10^9 p.f.u. Ad-sVEGFR3 before and 10 days after UUO.[3] Ad-β-galactosidase (10^9 p.f.u.) was used as a control. Ad-sVEGFR-3 and Ad-β-galactosidase were provided by Dr Gou Young Koh (Korea Advanced Institute of Science and Technology, DaeJeon, Republic of Korea).

Cells and reagents

For bone marrow–derived macrophages, bone marrow was isolated from femurs and tibias of male C57BL/6 mice and cultured in Dulbecco's modified Eagle's medium supplemented with 10% fetal bovine serum and 30% L929 conditioned media. MPT cells were generously provided by Dr Lloyd G. Cantley (Yale University School of Medicine, New Haven, CT). Raw 264.7 and HK2 cells (ATCC, Manassas, VA) were cultured in Dulbecco's modified Eagle's medium. hLECs were obtained from Lonza (Basel, Switzerland). TGF-β1 was purchased from Sigma-Aldrich (St Louis, MO) and TNF-α from R&D Systems (Minneapolis, MN). Recombinant human VEGF-C and VEGF-D were purchased from R&D Systems.

Isolation of glomeruli and tubules for RNA extraction

Glomeruli were isolated using a modified method that was previously described.[39] One week after ureteral obstruction, male C57BL/6 mice (Orient Bio; 18–20 g body weight) were anesthetized with an intramuscular injection of ketamine (100 mg/kg) and xylazine (10 mg/kg). Kidneys were removed, chopped into 1 mm^3 pieces, and digested in collagenase (1 mg/ml collagenase A, 100 U/ml deoxyribonuclease I) at 37 °C for 30 min with gentle agitation. The cell suspension was then gently minced using a 100-μm mechanical sieve, which was then washed with 5 ml of phosphate-buffered saline (PBS). The filtered cells were suspended in 3 ml of PBS. The glomeruli were isolated with a micropipette under a light microscope. The isolated glomeruli and remaining cells were used as glomeruli and renal tubules for mRNA extraction, respectively.

Immunofluorescence

Immunofluorescence staining was performed as described previously.[40] For immunofluorescence studies, mouse kidneys fixed with 4% paraformaldehyde were cryoprotected in 10% sucrose in PBS (3 h at 4 °C), immersed in 20% sucrose/10% glycerol in PBS (overnight at 4 °C), and then frozen in OCT Tissue-Tek compound (VWR Scientific, Arlington Heights, IL) before preparing 10-μm-thick cryosections. Anti-PECAM-1 (Chemicon International, Temecula, CA), anti-VEGFR-3 (R&D Systems), anti-podoplanin (Santa Cruz Biotechnology, Santa Cruz, CA), anti-Prox-1 (Reliatech, Braunschweig, Germany), anti-Ki-67 (Thermo Fisher Scientific, Fremont, CA), anti-mouse F4/80 (eBioscience, SanDiego, CA), anti-aquaporin 1 (Santa Cruz Biotechnology), anti-iNOS (BD Transduction Laboratories, San Jose, CA), and anti-VEGF-C antibodies (Invitrogen, Carlsbad, CA) were used for mouse kidney frozen sections. Secondary Alexa Fluor 488– or Alexa Fluor 555–conjugated antibodies to rat, rabbit, or hamster immunoglobulins (1:1000; Invitrogen) were used to visualize antigen–antibody complexes. Nuclei were stained with DAPI (4',6-diamidino-2-phenylindole). Digital images were obtained with a Zeiss Z1 microscope and a Zeiss LSM 510 confocal microscope (Carl Zeiss, Göttingen, Germany).

Histology and morphometric analysis of lymphatic vessels

Human and mouse kidneys were fixed in 10% neutral buffered formalin and embedded in paraffin. Kidney sections were histologically

evaluated with hematoxylin and eosin stain. The presence of interstitial fibrosis in human and mouse kidney section was assessed with Masson's trichrome stain using a method that we used earlier.[22] The positive area of Masson's trichrome stain was evaluated from the unit area and expressed as a percentage per unit area using a digital image analysis program (AnalySIS, Soft Imaging System, Münster, Germany). For each kidney section, five randomly selected nonoverlapping fields were analyzed. The number of lymphatic vessels per unit area was measured with a modification of methods previously described.[41] In brief, five individual fields per kidney section were examined at $\times 200$ magnication, and the number of vessels per unit area (0.45 mm $\times$ 0.45 mm) was determined.

Immunohistochemistry

For immunohistochemistry, kidneys were fixed overnight in 4% paraformaldehyde and embedded in paraffin. Four-micrometer sections were cut, dewaxed, and dehydrated. Endogenous peroxidase activity was blocked with 0.3% hydrogen peroxide in methanol for 30 min. Next, antigen retrieval was performed with a mixture of 2 mol/l HCl and 0.2% Triton X-100 in Tris-buffered saline for 30 min at room temperature. Slides were blocked with 10% normal goat serum and 1% bovine serum albumin in PBS for 15 min, and subsequently incubated overnight with primary antibodies against anti-D2-40 (Covance, Princeton, NJ) and LYVE-1 (AngioBio, Del Mar, CA). Slides were washed three times with Tris-buffered saline between the antibody incubations. Visualization was performed with 3-amino-9-ethyl carbazole (Dako, Carpinteria, CA) chromogenic substrate. Subsequently, the slides were counterstained with hematoxylin. The positive area of LYVE-1 was evaluated from the unit area (0.22 μm^2) and expressed as a percentage per unit area using a digital image analysis program (AnalySIS, Soft Imaging System).

Quantitative real-time RT-PCR

Total RNA was extracted from the kidney homogenates using Trizol (Invitrogen). The Transcriptor First Strand cDNA Synthesis Kit (Roche, Mannheim, Germany) was used to synthesize cDNA from total RNA according to the manufacturer's protocol. Quantitative real-time RT-PCR of mouse Ang1, Ang2, VEGF-A, VEGF-B, VEGF-C, and VEGF-D from kidney was performed in a 7900HT Fast Real-Time PCR System (Applied Biosystems, Carlsbad, CA). A 10-fold dilution of each cDNA was amplified in a 10 µl volume, using the SYBR Green PCR Master Mix (Applied Biosystems), with 200 nmol/l final concentrations of each primer (Supplementary Table S1 online). The PCR program was as follows: 10 min at 95 °C, then 95 °C for 10 s, and 60 °C for 30 s for 50 cycles. To confirm the use of equal amounts of RNA in each reaction, all samples were checked in parallel for glyceraldehyde 3-phosphate dehydrogenase mRNA expression. Supplementary Table S1 summarizes the primer sequences of mouse Ang1, Ang2, VEGF-A, VEGF-B, VEGF-C, and VEGF-D, and glyceraldehyde 3-phosphate dehydrogenase.

Depletion of macrophages with clodronate treatment and blockade of VEGF-C

Clodronate was purchased from Sigma and liposome-encapsulated clodronate was prepared according to previously described methods.[42] For systemic depletion of macrophages, clodronate liposome (50 mg/kg) was administered through the peritoneum 1 day before operation and every second day before collecting the kidney sample.[4] Empty control liposome was injected as a control.

Immunoblotting

Immunoblotting was performed as previously described.[21] Bone marrow–derived macrophages, Raw 264.7 cells, MPT cells, and HK2 cells were homogenized, and immunoblot analysis of protein expression was carried out using routine procedures. The primary antibodies to VEGF-C and arginase-1 (Abcam, Cambridge, MA) and iNOS (Santa Cruz) were used. The results of densitometric analyses are reported as the relative ratio to actin. The relative ratio measured in bone marrow–derived macrophages, Raw 264.7 cells, MPT cells, and HK2 cells treated with control buffer is arbitrarily presented as 1.

Capillary-like tube formation assay

In vitro tube formation assay was performed in a three-dimensional culture of hLECs on ECM gel (Sigma-Aldrich).[43]

Migration assay

The migration assay with hLECs was performed using a modified Boyden chamber (NeuroProbe, Cabin John, MD) as described previously.[43]

Cell proliferation by XTT assay

Proliferation of hLECs was measured using a Cell Proliferation Kit II (XTT; Roche) in accordance with the manufacturer's protocol.

Enzyme-linked immunosorbent assay

VEGF-C and VEGF-D were measured using an enzyme-linked immunosorbent assay kit in accordance with the manufacturer's protocol.

Statistical analysis

Data are means ± s.d. Student's *t*-test between two groups was performed to compare the means of normally distributed continuous variables. Comparison between three groups was performed by one-way analysis of variance followed by Dunnett's comparison test. The association between variables has been tested by Pearson's correlation. Statistical significance was set at $P < 0.05$.

DISCLOSURE

All the authors declared no competing interests.

ACKNOWLEDGMENTS

This study was supported by a grant of the Korea Healthcare Technology R&D Project, Ministry for Health, Welfare & Family Affairs, Republic of Korea (A091087).

SUPPLEMENTARY MATERIAL

Table S1. Primers for quantitative real-time PCR.
Figure S1. Recombination of sagittal images in sham-operated (a) and UUO kidney 1 (b), 2 (c), and 4 weeks (d) after obstruction.
Figure S2. Immunofluorescence study of LYVE-1, VEGFR-3, podoplanin, and Prox-1 in kidney.
Figure S3. Effect of adoptive VEGF-C-knockdown macrophage transfer on lymphangiogenesis in UUO kidney.
Figure S4. Tissue level of TGF-β1.
Figure S5. Immunoblot analyses of VEGF-C in Raw 264.7 cells.
Figure S6. Immunohistochemistry for D2-40, hematoxylin and eosin, and Masson's trichrome stain on normal and fibrotic kidney sections from patient with ureteral obstruction due to ureteral cancer.
Supplementary material is linked to the online version of the paper at http://www.nature.com/ki

REFERENCES

1. Aukland K, Bogusky RT, Renkin EM. Renal cortical interstitium and fluid absorption by peritubular capillaries. *Am J Physiol* 1994; **266**: F175–F184.
2. Baluk P, Tammela T, Ator E *et al.* Pathogenesis of persistent lymphatic vessel hyperplasia in chronic airway inflammation. *J Clin Invest* 2005; **115**: 247–257.
3. Kataru RP, Jung K, Jang C *et al.* Critical role of CD11b+ macrophages and VEGF in inflammatory lymphangiogenesis, antigen clearance, and inflammation resolution. *Blood* 2009; **113**: 5650–5659.
4. Kang S, Lee SP, Kim KE *et al.* Toll-like receptor 4 in lymphatic endothelial cells contributes to LPS-induced lymphangiogenesis by chemotactic recruitment of macrophages. *Blood* 2009; **113**: 2605–2613.
5. Kim KE, Koh YJ, Jeon BH *et al.* Role of CD11b+ macrophages in intraperitoneal lipopolysaccharide-induced aberrant lymphangiogenesis and lymphatic function in the diaphragm. *Am J Pathol* 2009; **175**: 1733–1745.
6. Maruyama K, Ii M, Cursiefen C *et al.* Inflammation-induced lymphangiogenesis in the cornea arises from CD11b-positive macrophages. *J Clin Invest* 2005; **115**: 2363–2372.
7. Cursiefen C, Chen L, Borges LP *et al.* VEGF-A stimulates lymphangiogenesis and hemangiogenesis in inflammatory neovascularization via macrophage recruitment. *J Clin Invest* 2004; **113**: 1040–1050.
8. El-Chemaly S, Malide D, Zudaire E *et al.* Abnormal lymphangiogenesis in idiopathic pulmonary fibrosis with insights into cellular and molecular mechanisms. *Proc Natl Acad Sci USA* 2009; **106**: 3958–3963.
9. Kerjaschki D, Regele HM, Moosberger I *et al.* Lymphatic neoangiogenesis in human kidney transplants is associated with immunologically active lymphocytic infiltrates. *J Am Soc Nephrol* 2004; **15**: 603–612.
10. Matsui K, Nagy-Bojarsky K, Laakkonen P *et al.* Lymphatic microvessels in the rat remnant kidney model of renal fibrosis: aminopeptidase p and podoplanin are discriminatory markers for endothelial cells of blood and lymphatic vessels. *J Am Soc Nephrol* 2003; **14**: 1981–1989.
11. Saaristo A, Veikkola T, Enholm B *et al.* Adenoviral VEGF-C overexpression induces blood vessel enlargement, tortuosity, and leakiness but no sprouting angiogenesis in the skin or mucous membranes. *FASEB J* 2002; **16**: 1041–1049.
12. Achen MG, Jeltsch M, Kukk E *et al.* Vascular endothelial growth factor D (VEGF-D) is a ligand for the tyrosine kinases VEGF receptor 2 (Flk1) and VEGF receptor 3 (Flt4). *Proc Natl Acad Sci USA* 1998; **95**: 548–553.
13. Morisada T, Oike Y, Yamada Y *et al.* Angiopoietin-1 promotes LYVE-1-positive lymphatic vessel formation. *Blood* 2005; **105**: 4649–4656.
14. Gale NW, Thurston G, Hackett SF *et al.* Angiopoietin-2 is required for postnatal angiogenesis and lymphatic patterning, and only the latter role is rescued by angiopoietin-1. *Dev Cell* 2002; **3**: 411–423.
15. Maisonpierre PC, Suri C, Jones PF *et al.* Angiopoietin-2, a natural antagonist for Tie2 that disrupts *in vivo* angiogenesis. *Science* 1997; **277**: 55–60.
16. Zhang F, Tang Z, Hou X *et al.* VEGF-B is dispensable for blood vessel growth but critical for their survival, and VEGF-B targeting inhibits pathological angiogenesis. *Proc Natl Acad Sci USA* 2009; **106**: 6152–6157.
17. Wu WK, Llewellyn OP, Bates DO *et al.* IL-10 regulation of macrophage VEGF production is dependent on macrophage polarisation and hypoxia. *Immunobiology* 2010; **215**: 796–803.
18. Mantovani A, Romero P, Palucka AK *et al.* Tumour immunity: effector response to tumour and role of the microenvironment. *Lancet* 2008; **371**: 771–783.
19. Kurahara H, Shinchi H, Mataki Y *et al.* Significance of M2-polarized tumor-associated macrophage in pancreatic cancer. *J Surg Res* 2011; **167**: e211–e219.
20. Guo G, Morrissey J, McCracken R *et al.* Role of TNFR1 and TNFR2 receptors in tubulointerstitial fibrosis of obstructive nephropathy. *Am J Physiol* 1999; **277**: F766–F772.
21. Kim W, Moon SO, Lee SY *et al.* COMP-angiopoietin-1 ameliorates renal fibrosis in a unilateral ureteral obstruction model. *J Am Soc Nephrol* 2006; **17**: 2474–2483.
22. Morimoto Y, Gai Z, Tanishima H *et al.* TNF-alpha deficiency accelerates renal tubular interstitial fibrosis in the late stage of ureteral obstruction. *Exp Mol Pathol* 2008; **85**: 207–213.
23. Hwang JS, Park EY, Kim WY *et al.* Expression of OAT1 and OAT3 in differentiating proximal tubules of the mouse kidney. *Histol Histopathol* 2010; **25**: 33–44.
24. Sabolic I, Valenti G, Verbavatz JM *et al.* Localization of the CHIP28 water channel in rat kidney. *Am J Physiol* 1992; **263**: C1225–C1233.
25. Clavin NW, Avraham T, Fernandez J *et al.* TGF-beta1 is a negative regulator of lymphatic regeneration during wound repair. *Am J Physiol Heart Circ Physiol* 2008; **295**: H2113–H2127.
26. Oka M, Iwata C, Suzuki HI *et al.* Inhibition of endogenous TGF-beta signaling enhances lymphangiogenesis. *Blood* 2008; **111**: 4571–4579.
27. Avraham T, Daluvoy S, Zampell J *et al.* Blockade of transforming growth factor-beta1 accelerates lymphatic regeneration during wound repair. *Am J Pathol* 2010; **177**: 3202–3214.
28. Joukov V, Pajusola K, Kaipainen A *et al.* A novel vascular endothelial growth factor, VEGF-C, is a ligand for the Flt4 (VEGFR-3) and KDR (VEGFR-2) receptor tyrosine kinases. *EMBO J* 1996; **15**: 290–298.
29. Makinen T, Jussila L, Veikkola T *et al.* Inhibition of lymphangiogenesis with resulting lymphedema in transgenic mice expressing soluble VEGF receptor-3. *Nat Med* 2001; **7**: 199–205.
30. Jeon BH, Jang C, Han J *et al.* Profound but dysfunctional lymphangiogenesis via vascular endothelial growth factor ligands from CD11b+ macrophages in advanced ovarian cancer. *Cancer Res* 2008; **68**: 1100–1109.
31. Naruse T, Yuzawa Y, Akahori T *et al.* P-selectin-dependent macrophage migration into the tubulointerstitium in unilateral ureteral obstruction. *Kidney Int* 2002; **62**: 94–105.
32. Sakamoto I, Ito Y, Mizuno M *et al.* Lymphatic vessels develop during tubulointerstitial fibrosis. *Kidney Int* 2009; **75**: 828–838.
33. Redente EF, Higgins DM, Dwyer-Nield LD *et al.* Differential polarization of alveolar macrophages and bone marrow-derived monocytes following chemically and pathogen-induced chronic lung inflammation. *J Leukoc Biol* 2010; **88**: 159–168.
34. Kawanishi N, Yano H, Yokogawa Y *et al.* Exercise training inhibits inflammation in adipose tissue via both suppression of macrophage infiltration and acceleration of phenotypic switching from M1 to M2 macrophages in high-fat-diet-induced obese mice. *Exerc Immunol Rev* 2010; **16**: 105–118.
35. Zampell JC, Avraham T, Yoder N *et al.* Lymphatic function is regulated by a coordinated expression of lymphangiogenic and anti-lymphangiogenic cytokines. *Am J Physiol Cell Physiol* 2012; **302**: C392–C404.
36. Chevalier RL, Forbes MS, Thornhill BA. Ureteral obstruction as a model of renal interstitial fibrosis and obstructive nephropathy. *Kidney Int* 2009; **75**: 1145–1152.
37. Zhang T, Guan G, Liu G *et al.* Disturbance of lymph circulation develops renal fibrosis in rats with or without contralateral nephrectomy. *Nephrology (Carlton)* 2008; **13**: 128–138.
38. Avraham T, Clavin NW, Daluvoy SV *et al.* Fibrosis is a key inhibitor of lymphatic regeneration. *Plast Reconstr Surg* 2009; **124**: 438–450.
39. Curat CA, Vogel WF. Discoidin domain receptor 1 controls growth and adhesion of mesangial cells. *J Am Soc Nephrol* 2002; **13**: 2648–2656.
40. Jung YJ, Kim DH, Lee AS *et al.* Peritubular capillary preservation with COMP-angiopoietin-1 decreases ischemia-reperfusion-induced acute kidney injury. *Am J Physiol Renal Physiol* 2009; **297**: F952–F960.
41. Lange-Asschenfeldt B, Weninger W, Velasco P *et al.* Increased and prolonged inflammation and angiogenesis in delayed-type hypersensitivity reactions elicited in the skin of thrombospondin-2—deficient mice. *Blood* 2002; **99**: 538–545.
42. Van Rooijen N, Sanders A. Liposome mediated depletion of macrophages: mechanism of action, preparation of liposomes and applications. *J Immunol Methods* 1994; **174**: 83–93.
43. Lee AS, Kim DH, Lee JE *et al.* Erythropoietin induces lymph node lymphangiogenesis and lymph node tumor metastasis. *Cancer Res* 2011; **71**: 4506–4517.